PROC. OF JSCE
No. 296, April 1980

THE EFFECT OF PLANE AND BED FORMS OF CHANNELS UPON THE MEANDER DEVELOPMENT

By Kazuyoshi HASEGAWA and Isao YAMAOKA***

1. INTRODUCTION

The flow in river bends or meanders and the channel deformation due to flow are very important problems in fluvial engineerings, but theoretical studies in these fields have not so much been promoted as those on fluvial theories in straight channels.

Recently, Engelund (1974) investigated the flow and bed topography in circular and variable-curvature bends, and derived the solutions for secondary flows within the vertical plane and the horizontal plane, respectively. Furthermore Engelund (1975) presented the instability theory of flow in curved alluvial channels, using a closed annular flume. On the other hand, Ikeda et al. (1976) proposed an assumption such that concentrations of flow due to bends near the concave bank lead to the extension of the meander channel, or the occurrence of deviation from the mean flow at the top of the concave bank is a necessary requirement for the meander development. Under this assumption they derived the critical wave length for meander development by use of their solution to the deviation of flow.

It is surely remarkable that the effect on the flow due to bends was taken into consideration directly in their derivation, but it seems to be insufficient that they paid less attention to the effect due to bed configurations. According to many observations of experiments and fields by Kinoshita (1957) and others, it is known that the meandering of streams is caused by the formation of alternating bars on the bed.

In this paper the approximate solutions for the flow effected by both channel bends and bed configurations are dealt with, and consequently some original diagrams expressing the developing regions for meandering curvatures in stream channels are proposed under the same assumption as Ikeda et al. adopted.

The results are verified in an experimental meandering flume with one side wall fixed and the other erodible.

* Research Associate, Dept. of Civil Engineering, Hokkaido University.
** Professor, Dept. of Civil Engineering, Hokkaido University.

2. FLOW ON ALTERNATING BARS IN THE MEANDERING CHANNEL

Hayashi (1970) proposed a solution for the flow on alternating bars in a straight channel by means of the potential-flow model, while, as mentioned above, Engelund (1974) derived solutions for the flow in fully developed meander bends using the shallow-water model. However, the Hayashi solution is hardly applicable to meandering channels because of the potential-flow theory used, and the Engelund solution does not effectively express the properties of the flow deflected by geometrical elements of the channel bed, because the inertia terms of the transverse component of a flow equation are eliminated. The present analysis is intended to fully take into account the flow pattern associated with the alternately undulating beds, and hence an inertia term of transverse components of the flow equation is to be preserved.

(1) Basic Equations

We consider the flow in a curved channel of which walls are vertical, the width is uniform, the bed is movable, and the flow is taken to be quasi-steady. We introduce a curvilinear co-ordinate system with the s-axis along the center line in the flow direction and the n-axis perpendicular to the channel, as shown in **Fig. 1** (a). It is assumed that the depth is small enough and the radius of curvature is large enough compared with the width. Then, s- and n-direction components of the equation of motion, and the equation of continuity, respectively, are written as

$$\frac{\rho}{\rho+n}U\frac{\partial U}{\partial s}+V\frac{\partial U}{\partial n}+\frac{UV}{\rho+n}=-\frac{\rho}{\rho+n}\frac{\partial(g\Xi)}{\partial s}-\frac{fU^2}{2H} \quad\cdots\cdots\cdots\cdots(1)$$

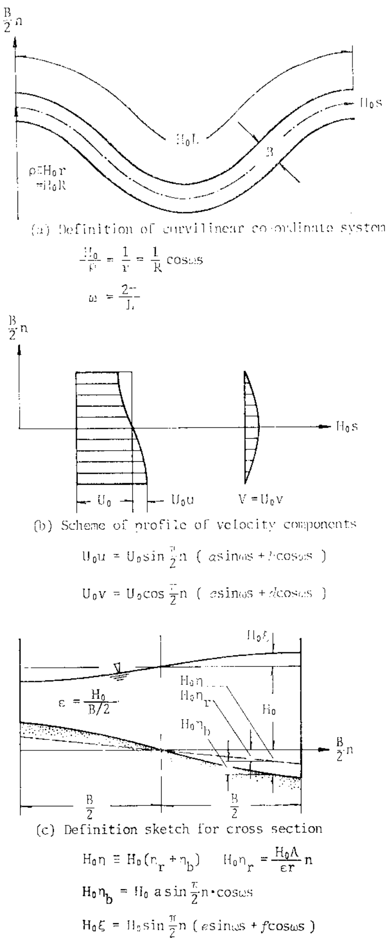

Fig. 1

$$\frac{\rho}{\rho+n}U\frac{\partial V}{\partial s}+V\frac{\partial V}{\partial n}-\frac{U^2}{\rho+n}=-\frac{\partial(g\Xi)}{\partial n}\cdots(2)$$

$$\frac{\rho}{\rho+n}\frac{\partial(HU)}{\partial s}+\frac{\partial(HV)}{\partial n}+\frac{HV}{\rho+n}=0\cdots\cdots(3)$$

where U and V=flow velocity components in the s and n directions averaged over the depth, respectively, H=water depth at any point, Ξ=surface level from the datum line, ρ=radius of curvature along the center line at any point, g=acceleration of gravity, and f=friction factor.

In order to linearize the equations, we make use of the following substitutions.

$$U=U_0(1+u)\cdots\cdots(4)$$

$$V=U_0 v\cdots\cdots(5)$$

$$H=H_0(1+\xi+\eta)\cdots\cdots(6)$$

$$\Xi=\Xi_0+H_0\xi\cdots\cdots(7)$$

$$\rho=H_0 r\cdots\cdots(8)$$

where the variable with subscript 0 stands for the one in a steady and uniform state, u is the velocity deviated from mean velocity, ξ and η are the displacements of the water surface and the bed, respectively, and u, v, ξ, and η are assumed to be small quantities. The distances along the s and n axes are normalized by H_0 and $B/2$ (B=channel width), respectively and hereafter for notational convenience the same characters of s and n are used. From (1) the equation in a steady-uniform state is derived as follows :

$$0=-\frac{\partial(g\Xi_0)}{\partial s}-\frac{\rho+n}{\rho}\frac{fU_0^2}{2H_0}\cdots\cdots(9)$$

By substitution of (4)～(9) into (1)～(3) we can obtain the first-order differential equations as follows:

$$\frac{\partial u}{\partial s}+\frac{1}{F^2}\frac{\partial\xi}{\partial s}+f\left[u-\frac{1}{2}(\xi+\eta)\right]=0\cdots\cdots(1)'$$

$$\frac{\partial v}{\partial s}+\frac{\varepsilon}{F^2}\frac{\partial\xi}{\partial n}-\frac{1}{r}=0\cdots\cdots(2)'$$

$$\frac{\partial u}{\partial s}+\frac{\partial\xi}{\partial s}+\varepsilon\frac{\partial v}{\partial n}+\frac{\partial\eta}{\partial s}=0\cdots\cdots(3)'$$

where $\varepsilon=2H_0/B$ and $F=U_0/\sqrt{gH_0}$.

Equations (1)′, (2)′ and (3)′ are the basic equations for the present analysis, which differ from those used by Engelund to the effect that the inertia term of $\partial v/\partial s$ is preserved in (2)′. This term may be neglected in a fully developed sinuous flow which is to be kept in an equilibrium state, but it must not be neglected in such a transitional flow as running over alternating bars. Equation (2)′ indicates that the difference between the centrifugal force and the transverse component of the momentum transported from the main flow is balanced by the radial surface inclination. If the inertia term is neglected in (2)′, the solution for u may easily be obtained by integrating (2)′ with respect to n and substituting a resulting equation into (1)′.

We need to introduce appropriate expressions for r and η to solve (1)′～(3)′. For r, Engelund adopted the expression proposed by Langbein and Leopold (1966) :

$$\frac{1}{r}=\frac{1}{R}\cos\frac{2\pi}{L}s=\frac{1}{R}\cos\omega s\cdots\cdots(10)$$

where R=minimum value of r, L=meander wave length normalized by H_0, and ω=wave number. Equation (10) is known as the "sine-generated curve" equation and this curve fits well the center lines of natural meandering rivers within about one wave length of them. We also follow the Engelund approach in the present analysis. The displacement of beds, η consists of the two components; one is alternating bar and the other is bed configuration due to bends. Alternating bars observed in laboratory flumes as well as in natural rivers are not always kept in regular configurations and sometimes their wave length is different from the channel wave length. However, according to Kinoshita (1961) the meander pattern that has two alternating bars within each meander wave is widely observed in Japanese alluvial rivers. In this pattern, the fronts of bars tend to arc-wise stretch in the direction of the concave banks and the procession of bars tends to stop, and therefore the wave length of the bed undulation almost equals that of plane form. On the contrary, the behavior of the bars in other patterns which have three or more within each meander wave has been less known. Thus, we limit the discussion on the flow for the meander pattern with two alternating bars, which will also be of practical importance.

A typical and simplified expression is desirable to find the fundamental effect on the flow due to η and hence, we adopt the following form :

$$\eta_b = a \sin\frac{\pi}{2}n.\cos\omega s \cdots\cdots\cdots\cdots\cdots\cdots\cdots\cdots\cdots\cdots (11)$$

where η_b=displacement caused by alternating bars, and a=wave height of the alternating bar normalized by H_0.

On the other hand, there occurs the scouring of beds caused by the secondary flow in curved channels, and then an equilibrium transverse bed slope inclined toward the outer bank is formed. As an approximate expression of these bed forms, Ikeda et al. (1976) proposed

$$\eta_r = \left(\frac{r+n/\varepsilon}{r}\right)^A - 1 \simeq A\frac{n}{\varepsilon r} \cdots\cdots\cdots\cdots\cdots\cdots (12)$$

where η_r=displacement caused by the scouring of beds, A=factor varying with the nondimensional tractive force and a velocity factor, and so on. From (10)～(12), the η can be expressed as

$$\eta = \eta_b + \eta_r = \left(a \sin\frac{\pi}{2}n + A\frac{n}{\varepsilon R}\right)\cos\omega s \cdots\cdots (13)$$

(2) Solution of the Basic Equations by the Method of Weighted Residuals (MWR)

We may hardly derive the rigorous solution to the basic equations, (1)′～(3)′. However, we can obtain the approximate solution using Galerkin's method (1972), which is one of the MWR techniques; the Galerkin method is of use to give rise to the approximate solutions analytically, instead of numerically. First, we have to choose the suitable trial functions for u, v, and ξ so as to satisfy the boundary conditions and to describe the phenomena of interest adequately. According to the observation of flows in curved channels, it appears that u and ξ are distributed as an odd function, while v as an even function. The v vanishes on the side walls and u, v, and ξ vary periodically in the s direction. Hence, as the trial functions in the n direction u and ξ will take $\sin\frac{\pi}{2}n$, while v takes $\cos\frac{\pi}{2}n$. On the other hand, as the trial functions in the s direction, $\sin\omega s$ and $\cos\omega s$ may be adequate for u, v, and ξ. As a result, we can choose the approximate solutions in the following forms :

$$u = \sin\frac{\pi}{2}n(\boldsymbol{a}\sin\omega s + \boldsymbol{b}\cos\omega s) \cdots\cdots\cdots (14.1)$$

$$v = \cos\frac{\pi}{2}n(\boldsymbol{c}\sin\omega s + \boldsymbol{d}\cos\omega s) \cdots\cdots\cdots (14.2)$$

$$\xi = \sin\frac{\pi}{2}n(\boldsymbol{e}\sin\omega s + \boldsymbol{f}\cos\omega s) \cdots\cdots\cdots (14.3)$$

where $\boldsymbol{a}$, $\boldsymbol{b}$, $\boldsymbol{c}$, $\boldsymbol{d}$, $\boldsymbol{e}$, and $\boldsymbol{f}$ are unknown coefficients to be determined. The steps required to implement the MWR involve (a) calculating the residuals by substituting the above approximations into the left-hand side of the equations, (1′)～(3)′, (b) integrating the weighted residuals multiplied by the trial functions and then setting the resulting equations equal to zero, and (c) solving the simultaneous equations for the coefficients of $\boldsymbol{a}$～$\boldsymbol{f}$ as follows :

$$\begin{bmatrix} f & -\omega & 0 & 0 & -\frac{f}{2} & -\frac{\omega}{F^2} \\ 0 & 0 & 0 & \omega & -\frac{\pi\varepsilon}{2F^2} & 0 \\ 0 & \omega & \frac{\pi\varepsilon}{2} & 0 & 0 & \omega \\ \omega & f & 0 & 0 & \frac{\omega}{F^2} & -\frac{f}{2} \\ 0 & 0 & \omega & 0 & 0 & \frac{\pi\varepsilon}{2F^2} \\ \omega & 0 & 0 & -\frac{\pi\varepsilon}{2} & \omega & 0 \end{bmatrix} \begin{bmatrix} \boldsymbol{a} \\ \boldsymbol{b} \\ \boldsymbol{c} \\ \boldsymbol{d} \\ \boldsymbol{e} \\ \boldsymbol{f} \end{bmatrix} = \begin{bmatrix} 0 \\ 0 \\ -\omega\left(a+\frac{8A}{\pi^2\varepsilon R}\right) \\ \frac{f}{2}\left(a+\frac{8A}{\pi^2\varepsilon R}\right) \\ \frac{4}{\pi R} \\ 0 \end{bmatrix} \cdots\cdots (15)$$

We can obtain the first order approximations when using the derived coefficients of $\boldsymbol{a}$～$\boldsymbol{f}$ in (14.1)～(14.3). We may proceed into the second or higher order approximations to find out the more accurate solutions. However, the first order approximate solutions seem to be sufficient to gain an insight into the fundamental properties of the flow.

3. CONDITIONS FOR THE MEANDER DEVELOPMENT

Processions and extensions of meander channels are caused by the growth of the deviation, u from the mean velocity near the top of the concave bank as described above. The deviation of u is closely associated with a coefficient of $\boldsymbol{b}$, since the relation of $u=\boldsymbol{b}$ can hold at the top of the concave bank for $n=1$ and $s=mL$ (m=0, 1, 2, …) in (14.1). Therefore, it is expected that the meanders develop under the condition of $\boldsymbol{b}>0$. On the contrary, they decrease for the case of $\boldsymbol{b}<0$. Solving (15) for $\boldsymbol{b}$ reduces to

$$\boldsymbol{b} = b_{RAa}/\Delta \cdots\cdots\cdots\cdots\cdots\cdots\cdots\cdots\cdots\cdots\cdots (16)$$

where

$$\Delta = \omega^2[4(F^2-1)\omega^2 - (\pi\varepsilon)^2]^2 + f^2[6(F\omega)^2 - (\pi\varepsilon)^2]^2 \cdots\cdots\cdots\cdots (16.1)$$

$$b_{RAa} = \frac{4\varepsilon}{R}[8(F^2-1)\omega^4 - 2\{3f^2F^4 + (\pi\varepsilon)^2\}\omega^2 + (\pi\varepsilon fF)^2] + \left(\frac{a}{2} + \frac{4A}{\pi^2\varepsilon R}\right)$$

$$\times[32(F^2-1)\omega^6-8(\pi\varepsilon)^2\omega^4 -6(\pi\varepsilon f F\omega)^2+f^2(\pi\varepsilon)^4] \cdots\cdots\cdots (16.2)$$

It is clear from (16) that the sign of $\boldsymbol{b}$ depends upon that of b_{RAa} in (16.2), because of Δ in (16.1) being always positive.

Equation (16.2) consists of the three components which have an influence on $\boldsymbol{b}$, that is,

(i) The first square bracket of (16.2) expresses the effect on $\boldsymbol{b}$ due to the plane form of the channel.

(ii) The term, a, multiplied by the second square bracket expresses the effect on $\boldsymbol{b}$ due to alternating bars.

(iii) The term, A, multiplied by the second square bracket expresses the effect on $\boldsymbol{b}$ due to the bed form resulting from the scouring in the sections of bends.

Herein we give account of the typical cases of how each component of (i)～(iii) will exert an influence on $\boldsymbol{b}$.

(1) Conditions for the Occurrence of Positive Deviation due to Bends

When the channel is bended and the bed is flat, the a and A terms vanish, and therefore the deviation only occurs in the case of (i).

The requirement of $\boldsymbol{b}>0$ leads to the following constraints :

$$F^2{}_{R2}<F^2<F^2{}_{R1} \text{ and } \omega^2<\frac{\pi\varepsilon f}{4\sqrt{2}} \cdots (17.1)$$

$$F^2{}_{R2}<F^2<F^2{}_{R1} \text{ and } \omega^2>\frac{3}{2}f^2\left[\sqrt{\frac{2}{9}\left(\frac{\pi\varepsilon}{f}\right)^2+1}+1\right]\cdots (17.2)$$

where

$$\left.\begin{matrix}F^2{}_{R1}\\F^2{}_{R2}\end{matrix}\right\}=\frac{1}{12(f\omega)^2}[8\omega^4+(\pi\varepsilon f)^2 \pm\sqrt{64\omega^8-192f^2\omega^6-32(\pi\varepsilon f)^2\omega^4+(\pi\varepsilon f)^4}] \cdots\cdots (17.3)$$

For the particular case of $F^2 f\ll\pi\varepsilon$, which often occurs in natural rivers, (17.1) and (17.2) can reduce to

$$\omega<\frac{fF}{\sqrt{2}} \cdots\cdots\cdots (17.1)'$$

$$\omega>\frac{\pi\varepsilon}{2\sqrt{F^2-1}} \cdots\cdots\cdots (17.2)'$$

Equation (17.1)′ is identical with the condition for meander developments, derived by Ikeda. Equation (17.2)′ is a newly derived condition resulting from the present analysis. The diagrams indicating curvature-developing regions are shown in **Figs. 2～13** together with (17.1) and (17.2).

(2) Conditions for the Occurrence of Positive Deviation due to Bars

In the case of $1/R=0$ and $a\neq 0$, where the channel is straight and the bed has alternating bars, it is notable that the deviation occurs only in the above case of (ii). It suffices to consider that the positive deviation due to bars in a straight channel could occur at the top of the talweg. From the requirement of $\boldsymbol{b}>0$, we can find the following conditions:

$$F^2<F_a{}^2 \text{ and } \omega^2<\omega_{a1}{}^2\simeq\pi\varepsilon f/(2\sqrt{2}) \cdots\cdots (18.1)$$

$$F^2>F_a{}^2 \text{ and } \omega^2>\omega_{a2}{}^2=\sqrt{3}\pi\varepsilon f/4\cdots (18.2)$$

where

$$F_a{}^2=\frac{32\omega^6+8(\pi\varepsilon)^2\omega^4-f^2(\pi\varepsilon)^4}{2\omega^2[16\omega^4-3(\pi\varepsilon f)^2]} \cdots\cdots (18.3)$$

Hayashi (1976) presented the necessary condition under which the bars are formed as follows :

$$F^2<\frac{40(\pi\varepsilon)^2\omega^2+5(\pi\varepsilon)^4}{288\omega^4+[28(\pi\varepsilon)^2+72f^2]\omega^2-9(\pi\varepsilon f)^2} \cdots\cdots (19)$$

The condition of (18.2) is of less importance in the light of the necessary condition on the bar formation given by (19). The above equations are also shown in **Figs. 2～13**. It is obvious from the figures that ω varies slightly with F and the effect of εf on ω rather predominates over that of F. Therefore, (18.1) can approximately be expressed as

$$\omega<\omega_{a1}\simeq\sqrt{\pi\varepsilon f/(2\sqrt{2})}\simeq\sqrt{\varepsilon f}$$
(F is less than about 2) ……(18.1)′

It is of interest to note that the critical wave number for meander developments contains the depth-width ratio, ε.

(3) Conditions for the Occurrence of Positive Deviation due to Scoured Beds

When the channel is bended and the bed is in a scouring state, the term, a, vanishes, and then the deviation occurs for both cases of (i) and (iii). The condition of $\boldsymbol{b}>0$ leads to

$$F_{A2}{}^2<F^2<F_{A1}{}^2 \text{ and } \omega^2<\omega_{A1}{}^2 \simeq\frac{(\pi\varepsilon)^2}{8A}\left[\sqrt{8\left(\frac{Af}{\pi\varepsilon}\right)^2+1}-1\right]\cdots (20.1)$$

$$F_{A2}{}^2<F^2<F_{A1}{}^2 \text{ and } \omega^2>\omega_{A2}{}^2\simeq\sqrt{6}\pi\varepsilon f/4 \cdots\cdots (20.2)$$

where

$$\left.\begin{matrix}F_{A1}{}^2\\F_{A2}{}^2\end{matrix}\right\}=\frac{1}{2\alpha_A}[\beta_A\pm\sqrt{\beta_A{}^2-4\alpha_A\gamma_A}]\cdots (20.3)$$

$$\alpha_A=6(f\omega)^2$$

$$\beta_A=8\omega^4+(\pi\varepsilon f)^2+\frac{2A}{(\pi\varepsilon)^2}\omega^2[16\omega^4-3(\pi\varepsilon f)^2]$$

$$\gamma_A=8\omega^4+2(\pi\varepsilon\omega)^2+\frac{A}{(\pi\varepsilon)^2}[32\omega^6+8(\pi\varepsilon)^2\omega^4 -f^2(\pi\varepsilon)^4]$$

The conditions of (20.1)～(20.2) are also indicated in **Figs. 2～13**, when using $A=10$.

It is found from the figures that Eq. (20) are plotted between Eq. (17) and (18). Equation (20) approaches Eq. (17) with the value of A decreasing, while they approach Eq. (18) with A increasing. Following the same procedure as for the derivation

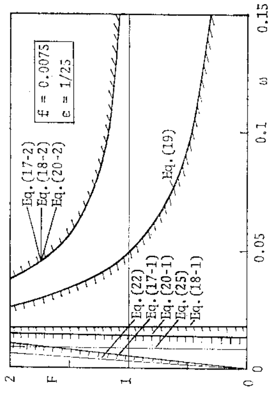

Fig. 2

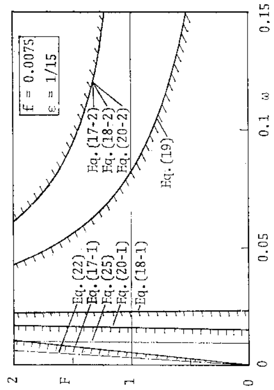

Fig. 3

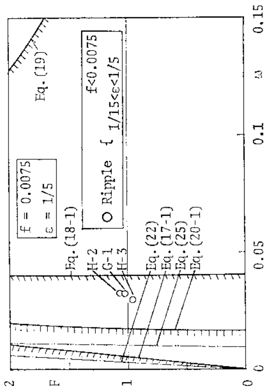

Fig. 4

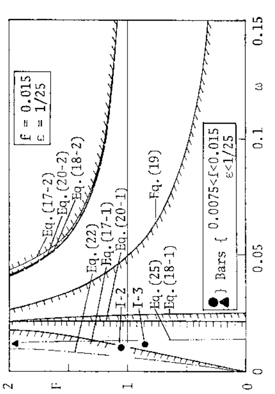

Fig. 5

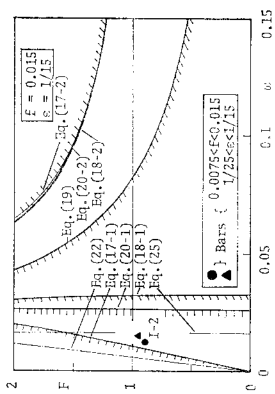

Fig. 6

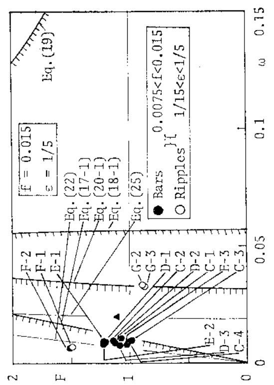

Fig. 7

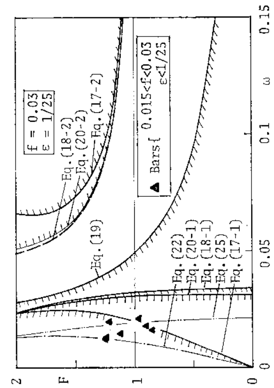

Fig. 8

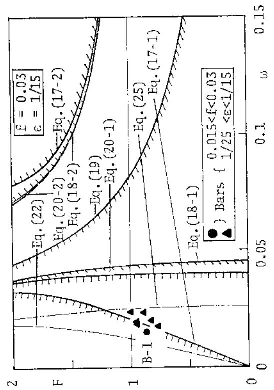

Fig. 9

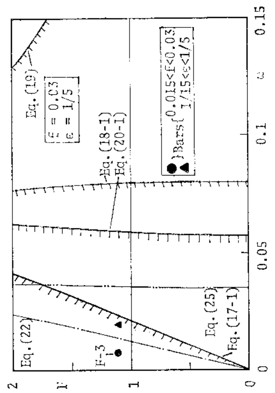

Fig. 10

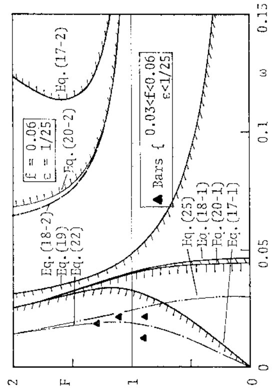

Fig. 11

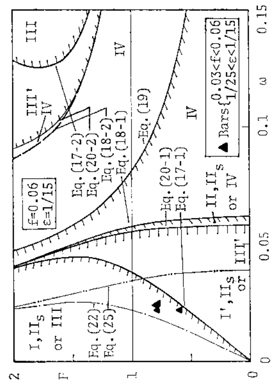

Fig. 12

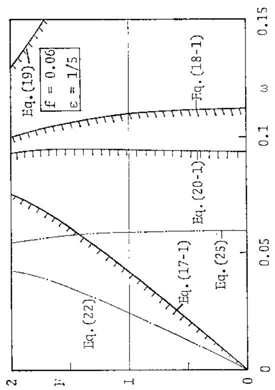

Fig. 13

Figs. 2~13 Diagram of curvature-developing regions.

of (18.1)′, we can obtain the approximate solution to (20.1) as

$$\omega < \omega_{A1} \simeq \frac{\varepsilon}{\sqrt{A}}\sqrt{\sqrt{\left(\frac{Af}{\varepsilon}\right)^2+1}-1} \cdots\cdots (20.1)'$$

The above conditions obtained are independent of the condition of (19), because we consider the case where no bars exist.

(4) Conditions for the Occurrence of Positive Deviation due to the Three Interactions

When the channel is bended and the bed is associated with alternating bars, the deviation occurs due to the interactions of (i), (ii), and (iii), and then the condition of (16.2) can be used without any change to find the condition of $\boldsymbol{b}>0$. However, the resulting equation is nearly equal to the conditions of Eqs. (18), since the component of (i) is considerably smaller than that of (ii) and can be neglected. It should be kept in mind that this condition is valid only for the case in which there are two alternating bars within each meander wave, and the wave length of the bed undulation is almost identical with that of plane form and no lags exist between both waves. On the other hand, it is anticipated that the deviations of flow due to bars and bends will be superposed with their different wave lengths for the meander pattern in which the length of bars is relatively short and different from the channel wave length. However, it is difficult to analytically derive the condition for the meander development under such a complex pattern, since the form of bars with a short wave length in the channel bend has not yet been known.

4. MAXIMUM DEVIATIONS FOR THE THREE CASES AND THEIR COMPARISONS

A similarity requirement should be considered between planimetric forms of channels of interest to find the maximum value of $\boldsymbol{b}$ with respect to ω. The minimum radius of curvature, R, cannot be regarded as constant in terms of ω. On the other hand, the maximum deviation angle $(=\theta_0)$ of the channel from the valley axis will be constant with respect to ω if a similarity condition is preserved. Hence, we need to find the relationship between R and θ_0. The deviation angle θ at any point, when integrating (10) for the s, is given by

$$\theta = \frac{1}{R_\omega}\sin\omega s \cdots\cdots (10)$$

The relationship between R and θ_0 is easily obatined by substituting $\theta=\theta_0 \sin\omega s$ into (10)′ as follows :

$$\frac{1}{R} = \theta_0 \omega \cdots\cdots (21)$$

We may use Eq. (21) for R in the subsequent analyses. It is worth while pointing out that the differentiation of (16) with respect to ω to find the maximum value of $\boldsymbol{b}$ is almost equivalent to that of the numerator of (16), because the denominator of (16) $(=\Delta)$ varies slightly and monotonously in terms of ω in the region considered.

(1) The Condition for the Maximum Deviation in the Case of (i)

The wave number, ω_{RP} at which the $\boldsymbol{b}$ has the maximum value is obtained by differentiating (16.2) with respect to ω and using $A=a=0$ as follows :

$$F^2 = \frac{1}{36(f\omega_{RP}{}^2)}[40\,\omega_{RP}{}^4 + (\pi\varepsilon f)^2 - \sqrt{1\,600\,\omega_{RP}{}^8 - 2\,880\,f^2\omega_{RP}{}^6 - 352(\pi\varepsilon f)^2\omega_{RP}{}^4 + (\pi\varepsilon f)^4}\,] \cdots\cdots (22)$$

The approximate solution to (22), when neglecting the higher order terms of ω_{RP}, is given by

$$\omega_{RP} \simeq \frac{fF}{\sqrt{6}} \cdots\cdots (22)'$$

This equation is identical with the dominant meander wave length derived by Ikeda. Equation (22) is indicated by a dot-dash line in **Figs. 2~13.**
When the derived wave number of ω_{RP} is substituted into (16) along with $a=A=0$ and the terms of f of orders higher than three are neglected, the maximum deviation of $\boldsymbol{b}_{RP}$ is given by

$$\boldsymbol{b}_{RP} = \frac{\frac{8}{3\sqrt{6}}\theta_0\varepsilon(\pi\varepsilon)^2(fF)^3}{\frac{1}{6}f^2(\pi\varepsilon)^4(F^2+6)} \cdots\cdots (23)$$

(2) The Condition for the Maximum Deviation in the Case of (ii)

The deviation $\boldsymbol{b}$ with respect to ω does not take the maximum value in the case of $1/R=0$, and the smaller ω is, the greater $\boldsymbol{b}$ becomes. In actual flows, however, the maximum deviation occurs at the corresponding wave length with which the growth rate of bars becomes maximum. Therefore, it is considered that the condition in this case will be decided from the theory of bar-formation, but this argument is beyond the scope of the present paper. Herein, for the purpose of comparing with (23), we obtain the deviation of $\boldsymbol{b}_a$, when using (22)′ and the condition of $1/R=0$ as follows :

$$\boldsymbol{b}_a = \frac{\frac{a}{2}f^2(\pi\varepsilon)^4}{\frac{1}{6}f^2(\pi\varepsilon)^4(F^2+6)} \cdots\cdots (24)$$

in which the terms of f of orders higher than three are neglected.

(3) The Condition for the Maximum Deviation in the Case of (iii)

By the same way as mentioned in the section of

4. (**1**), the wave number, ω_{AP} which gives the maximum deviation is found in an implicit form as

$$F^2=\frac{1}{2\alpha_{AP}}[\beta_{AP}-\sqrt{\beta_{AP}^2-4\alpha_{AP}\gamma_{AP}}]\cdots(25)$$

where

$$\alpha_{AP}=18(f\omega_{AP})^2$$

$$\beta_{AP}=40\,\omega_{AP}^4+(\pi\varepsilon f)^2+\frac{2A}{(\pi\varepsilon)^2}\omega_{AP}^2\{112\,\omega_{AP}^4-9(\pi\varepsilon f)^2\}$$

$$\gamma_{AP}=40\omega_{AP}^4+6(\pi\varepsilon\omega_{AP})^2+\frac{A}{(\pi\varepsilon)^2}\{224\,\omega_{AP}^6+40(\pi\varepsilon)^2\omega_{AP}^4-f^2(\pi\varepsilon)^4\}$$

Equation (25) is described by a two-dot-dash line in **Figs. 2~13**. The approximate solution for ω_{AP}, when neglecting the higher order terms of ω_{AP} and assuring that ω_{AP} little varies with F, is obtained by

$$\omega_{AP}\simeq\pi\varepsilon\sqrt{\frac{3}{40A}\left\{\sqrt{\frac{40}{9}\left(\frac{Af}{\pi\varepsilon}\right)^2+1}-1\right\}}\cdots\cdots(25)'$$

Equation (25)′ can furthermore reduce to

$$\text{when } \frac{40}{9}\left(\frac{Af}{\pi\varepsilon}\right)^2\ll 1 \text{ then } \omega_{AP}\simeq\sqrt{\frac{A}{6}}f\cdots\cdots(25.1)'$$

$$\text{when } \frac{40}{9}\left(\frac{Af}{\pi\varepsilon}\right)^2\gg 1 \text{ then } \omega_{AP}\simeq 0.705\sqrt{\varepsilon f}\cdots\cdots(25.2)'$$

(**4**) The Comparison of the Maximum Deviation due to Bends and Bars

Now the question arises as to which is the more essential factor to the occurrence and development of meanders, the plane form or the bed form. To answer this question, it is of interest to compare (23) with (24). The ratio of (23) to (24) yields

$$\frac{\boldsymbol{b}_{RP}}{\boldsymbol{b}_a}=\frac{16}{3\sqrt{6}}\frac{\theta_0}{\pi^2}\frac{fF^3}{a\varepsilon}\cdots\cdots(26)$$

Using abundant experimental data on fully developed alternating bars, Kuroki et al. (1975) proposed the relationship between the values of a and ε as

$$a=\frac{0.05}{\varepsilon}\cdots\cdots(27)$$

Substituting (27) into (26) gives

$$\frac{\boldsymbol{b}_{RP}}{\boldsymbol{b}_a}=4.41\,\theta_0 fF^3\cdots\cdots(26)'$$

The numerical value given by (26)′ is of order, about 10^{-1}, because the values of $\theta_0<\pi$, $F<1$, and $f\simeq 10^{-2}$ are often encountered in natural rivers.
It follows from this comparison that the effect of bends is rather negligible and the occurrence and development of meanders are caused mainly by the bed form such as alternating bars.

In the lower delta reaches of natural rivers, the alternating bars are seldom or not at all found on the beds, though the intensely sinuous state is often pronounced in the channels, according to Kinoshita (1957 and 1961) and other geomorphologists. This observation appears to contradict the fact as mentioned above, but we cannot deny the possibility that the meanders developed primarily by the effect of bars at the initial stage and then the bars disappeared as the hydraulic conditions changed, because the pattern observed at the present is the phase of the historical changes.

(**5**) The Comparison of the Maximum Deviation due to Scoured Beds and Bars

The ratio of $\boldsymbol{b}_A$, which is given by the use of $a=0$ in (16), to $\boldsymbol{b}_a$ for the case of $1/R=0$ is approximately written as

$$\frac{\boldsymbol{b}_A}{\boldsymbol{b}_a}=\frac{8\,\theta_0\omega}{\pi^2 a\varepsilon}\left[A-\frac{8(F^2-1)\omega^4-2(\pi\varepsilon)^2\omega^2+(\pi\varepsilon fF)^2}{8\,\omega^4+6(fF)^2\omega^2-(\pi\varepsilon f)^2}\right]\cdots\cdots(28)$$

When (25)′ and (27) are substituted into (28), we can obtain the ratio which gives rise to the maximum deviation due to scoured beds. When using typical values of $f=0.01$, $\varepsilon=1/15$, $A=10$ and $F=0.3$, which are often observed in natural rivers, the ratio comes to

$$\frac{\boldsymbol{b}_{AP}}{\boldsymbol{b}_a}=1.37\,\theta_0\cdots\cdots(29)$$

This result indicates that when the maximum deviation angle of θ_0 becomes around 42°, the effects on the deviation due to bends and bars are nearly identical.

5. CLASSIFICATION OF THE STATES OF ALLUVIAL CHANNELS

Alluvial rivers have various channel patterns and different states of channel deformation. These states can be classified on the basis of the combinations of the effects due to the bends and beds derived in the previous chapters, if we exclude the complicated patterns which have more than two alternating bars within each meander wave. For convenience the states can be classified into the seven referred to as I, II, ⋯, and so on, shown in the columns of **Table 1**, from the standpoint of whether or not the deviation is positive. The seven states under consideration are :

(I) the case in which the planimetric form, scoured bed, and bars altogether exert positive effects on the deviation.

(I′) the case in which both of the scoured bed and bars exert positive effects on the deviation.

(II) the case in which the planimetric and scoured bed exert no positive effects on the deviation in spite of the channel bending.

(II_s) the particular case of (II) in which the

Table 1 Classification for situations of alluvial rivers from the viewpoint of occurrence of velocity deviation.

Bed Configuration \ Effects due to Bars \ Effects due to Bends \ Plane forms of the channel		Meandering			Straight
		Due to both the plane form of bends and the scoured bed-form based on bends	Due to the scoured bed form based on bends	Not to be exerted	No bends
Alternating Bars	To be exerted	I	I′	II	II s
	Not to be exerted			IV	IV
Other Configurations 1) ripple, dunes 2) flat bed 3) transition	No bars	III	III′	IV	IV

channel is straight.

(III) the case in which no bars exist on the bed, and the planimetric form and scoured bed exert positive effects on the deviation.

(III′) the case in which no bars exist on the bed, and the scoured bed exerts a positive effect on the deviation.

(IV) the case in which no positive effects are exerted.

Fig. 12 shows a classification example of the states of alluvial channels. In this figure, the states of (III) and (III′) where no bars actually exist, are included in the region where the bars are formed, because the condition to form the bars derived by Hayashi is not a sufficient but a necessary condition. In this classification it is noted that meanders may develop in the cases of I, I′, II, III, and III′. The adequacy of this classification will be verified in the succeeding chapter by the measurements of the rate of width extension in the experiments carried out under a particular hydraulic condition corresponding to each state classified.

6. VERIFICATION BY EXPERIMENTS

(1) The Apparatus and Procedure

The outline of the flume used is illustrated in **Fig. 14**. The left-side wall of the flume is wooden and painted, and the right-side wall is made of erodible material, i.e., sand. The planimetric form of the fixed wall is given by a sine-generated curve as

$$\theta=\frac{\pi}{4}\sin\frac{2\pi}{422.7(\mathrm{cm})}s$$

and the length is equal to 8.5 meter (2 wave length).

The right-side wall and the bed of the flume are composed of the sand with a median diameter of $d_{50}=0.425$ mm and a specific gravity of 2.661, which are formed to a semitrapezoidal section by use of a scraper with the side angle of 30°. The bed slope is set flat in the direction of the valley axis and the flow is supplied by a circulation pump and measured with a calibrated orifice meter. The eighty stations for measurements are set up along the left-side wall at equal spaces in order from the most upper station, which are referred to as No. 1, 2, ⋯, etc.

The reach for measuring hydraulic variables is taken between No. 50 and No. 56, where the most intensive erosion of bank

Table 2 Experimental conditions and observed regions.

Run	Initiated Region	Discharge $Q(l/s)$	Bed Slope I	Channel-Width B(cm)	Mean Water Depth H_0(cm)	Observed Region
A	I	0.695	1/100	29.33 33.83 38.00	0.969 0.925 0.912	III I I
B	II	1.244	1/100	45.67 51.67	1.004 0.818	I I
C	III	0.290	1/139	13.33 14.00 14.67 16.50	0.707 0.657 0.671 0.606	I′ I′ I I
D	III	0.211	1/130	10.17 11.67 13.67	0.608 0.574 0.517	I′ I I
E	III	0.179	1/139	7.83 9.50 11.67	0.610 0.532 0.524	I′ I I
F	III	0.105	1/100	6.33 7.33 8.17	0.462 0.432 0.481	III I I
G	IV	2.770	1/300	23.83 27.00 27.50	2.198 2.247 2.205	IV IV IV
H	IV	3.000	1/300	21.50 24.33 31.83	2.418 2.206 2.006	IV IV IV
I	I′	0.785	1/200	37.27 38.93 40.13	0.809 0.696 0.796	I′ I′ I′

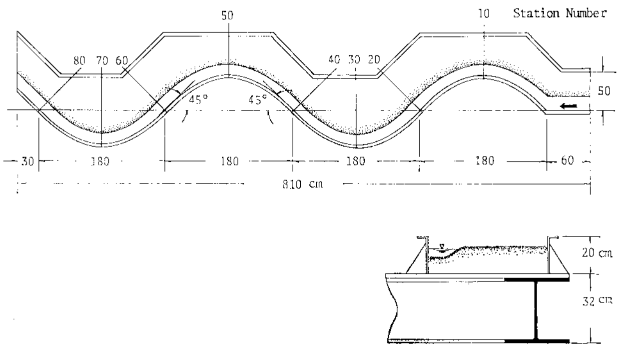

Fig. 14 Experimental flume.

would take place. The experiments carried out are shown in **Table 2**. The experiments were started under initiated regions indicated in the second column of **Table 2**, but at the end of the experiments we observed the regions shown in the last column of the table. The judgement of whether or not alternating bars were formed, was based upon the following equation (30), which was presented by Kuroki et al. (1975) and the photographs of bed configurations taken.

$$3\left(\frac{BI}{R_d}\right)^{0.5} > \frac{u_*}{u_{*c}} > 1.2\left(\frac{BI}{R_d}\right)^{0.5} \cdots\cdots\cdots\cdots (30)$$

where R_d=hydraulic depth, I=inclination of bed slope, and u_* and u_{*c}=friction velocity and its critical velocity, respectively. In every run, the procedures mentioned below were repeated 3 or 5 times, at the time intervals of 3～5 minutes in the rapid phenomena or 30～50 minutes in the sluggish phenomena.

Stopping the flow temporarily after the measurements of the transversal surface water profiles at the spaces of 20 mm, we measured the bed surface profile at the spaces of 5 mm by use of point gages, and took photographs to measure the rate of width extensions along the bank using a camera settled on a trolley.

(2) Results of Experiments

As the results of the experiments, Run A, B, C, D, E and F were classified into the region I, while Run G and H, and Run I, respectively, were classified into the region IV and I'. Run A and F were found in the region III at an early stage of experiments, but they transitionally changed to the region I.

These classifications were made in the following manner. The effects due to bends were classified by comparing the hydraulic variables resulting from the experiments with the conditions of Eqs. (17) and (20). The classification on the effect due to beds was performed by three successive ways; (1) The hydraulic variables were compared with the condition of Eq. (30). (2) The judgement was made on whether or not the bars had developed enough to exert actual effect on flows. This judgement was done by finding out whether the fronts of bars obviously developed, by means of observations during the experiments and examinations of the photographs. (3) The hydraulic variables were compared with the condition of Eq. (18). Therefore, some experiments in which the hydraulic variables satisfied Eq. (30), but the fronts of bars were not clearly found are classified into the region of no bars formed. These classifications were confirmed by plotting F and ω observed in each run in the corresponding figures of **Figs. 2～13**. The symbols of (●) and (○) plotted in these figures represent the bars which were fully developed and ripples or others, respectively.

The rate of extension of the channel width is shown in **Figs. 15～18**, in which some typical cases classified into each region are selected. The ordinate in the figures denotes the accumulation of the rate of width extensions obtained at each time inter-

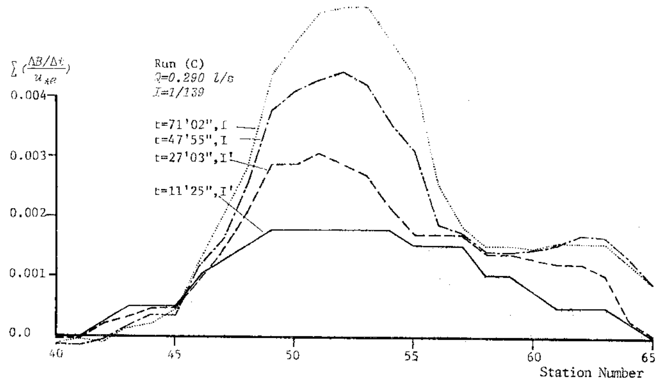

Fig. 15 Rate of width extension along the channel in Run (C).

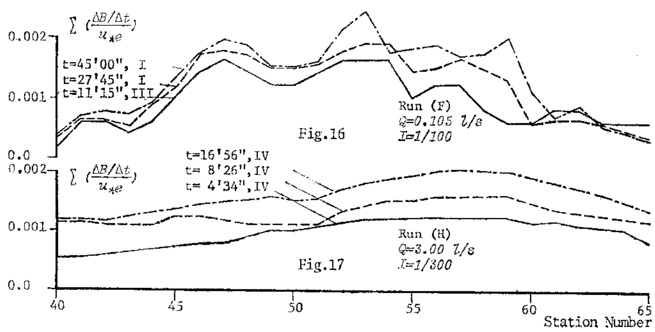

Figs. 16, 17 Rate of width extension along the channel in Run (F) and Run (H).

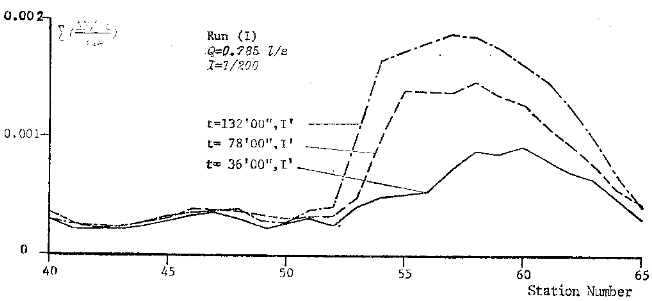

Fig. 18 Rate of width extension along the channel in Run (I).

val, and the abscissa denotes the station numbers. In the experiments classified into the region I, it is found in **Fig. 15** that there occurs an intensive erosion near the top of the concave bank (i.e., Station 50), and successive developments of the meander proceed. Run I classified into the region I′ also tends to follow a similar pattern as shown in **Fig. 18**. However, some fluctuations in the trend pattern are observed along the bend in Run E and F as shown in **Fig. 16**, in spite of that they are classified into the region I. The fluctuations are considered to be caused by independent exertion of bars having a shorter wave length different from the channel wave length. In contrast with the above observations, the bank erosion observed in Run G and H classified into the region Ⅳ, was found to be weak and uniform at any point of the channel so that any development of meanders was not recognized as shown in **Fig. 17**.

Analyzing the experimental results, it is found that the theoretically classified regions satisfactorily correspond to the regions judged from the hydraulic meandering phenomena observed in the present experiments. In addition, some of data which were obtained from the experiments on unconstrained meanders (i.e., "free meanders") carried out formerly in our laboratory are plotted in **Figs. 2～13** with the symbol of (▲) used. From the figures, all of data for free meanders lie within the region I and I′. These results also elucidate the validity of the theory developed.

7. SUMMARY

(1) The deviation of the velocity from the mean flow in a meandering channel having alternating bars on the bed was analyzed, and the three factors effecting the deviation were found. They are plane forms of the channel, scoured bed-forms due to channel bends, and configurations of alternating bars.

(2) It was obtained by the comparison of each effect that the effect due to plane forms is relatively small and practically negligible, and the effect due to scoured bed-forms possibly predominates over that due to bars in accordance with the intensity of the curvature.

(3) Alternating bars occur even in straight channels, and play an important role in causing the initial bends in the channel.

(4) New diagrams of curvature-developing regions in various cases having different combinations of the effects were proposed under the assumption that meanders develop when the deviation is positive at the top of the concave bank. Furthermore, it was shown that these regions could be applicable to the classification for the states of alluvial channels except for the meander pattern with more than two alternating bars.

(5) Some experiments classified into each region proposed were carried out, and the experimental results verify the validity of the theory the authors have proposed.

ACKNOWLEDGMENT

The authors would like to thank Mr. H. Itoh for his valuable help in 1978-1979 when he was a graduate student.

REFERENCES

1) Engelund, F. : Flow and bed topography in channel bends, Proc. of ASCE, Vol. 100, No. HY 11, 1631～1648, 1974.
2) Engelund, F. : Instability of flow in a curved alluvial channel, Jour. of Fluid Mech., Vol. 72, Part 1, 145～160, 1975.
3) Finlayson, B.A. : The Method of Weighted Residuals and Variational Principles, Academic Press, 1972.
4) Hayashi, T. : The formation of meanders in rivers, Proc. of JSCE, No. 180, 61～71 (in Japanese), 1970.
5) Hayashi, T. and S. Ozaki : On dominant wave length in river meanders from the viewpoint of stability theory on beds, Proc. of the 20th Japanese Conference on Hydraulics, 89～96 (in Japanese), 1976.
6) Ikeda, S., M. Hino and H. Kikkawa : Theoretical study on the free meandering of rivers, Proc. of JSCE, No. 255, 63～73 (in Japanese), 1976.
7) Kinoshita, R. : Formation of "Dune" on river beds—An observation on the condition of river meandering, Trans. of JSCE, No. 42, 1～21 (in Japanese), 1957.
8) Kinoshita, R. : Transitional Changes of Channels in the Ishikari Rivers, Report No. 36, Department of Natural Resources in the Agency of Science and Technology (in Japanese), 1961.
9) Kuroki, M., T. Kishi and T. Itakura : Hydraulic characteristics of alternating bars, "Studies on the bed configuration and roughness of alluvial rivers", Final research report of a grant in aid for scientific research from the Ministry of Education (in Japanese), 1975.
10) Langbein, W.B. and L.B. Leopold : River meanders—Theory of minimum variance, Geological Survey Prof. Paper 422-H, 1966.

(Received June 15, 1979)